Flexible Organic Memory Devices with Multilayer Graphene Electrodes

Yongsung Ji,[†,§] Sangchul Lee,[‡,§] Byungjin Cho,[†] Sunghoon Song,[†] and Takhee Lee[†,‡,*]

[†]School of Materials Science and Engineering [‡]Department of Nanobio Materials and Electronics Gwangju Institute of Science and Technology, Gwangju 500-712, Korea. [§]These authors equally contributed to this work.

ABSTRACT We fabricated 8 × 8 cross-bar array-type flexible organic resistive memory devices with transparent multilayer graphene (MLG) electrodes on a poly(ethylene terephthalate) substrate. The active layer of the memory devices is a composite of polyimide and 6-phenyl-C61 butyric acid methyl ester. The sheet resistance of the MLG film on memory device was found to be ~270 Ω/□, and the transmittance of separated MLG film from memory device was ~92%. The memory devices showed typical write-once-read-many (WORM) characteristics and an ON/OFF ratio of over ~10^6. The memory devices also exhibited outstanding cell-to-cell uniformity with flexibility. There was no substantial variation observed in the current levels of the WORM memory devices upon bending and bending cycling up to 10 000 times. A retention time of over 10^4 s was observed without fluctuation under bending.

KEYWORDS: organic resistive memory · flexible memory · graphene electrode

Organic electronics, such as organic light-emitting diodes, solar cells, transistors, and memory devices, have been intensively investigated to overcome several limits of inorganic-based electronics, such as complex fabrication processes, high cost, low throughput, and low flexibility.[1,2] Organic materials are good for large-area devices and exhibit high throughput due to their printability.[3,4] Furthermore, the elasticity and flexibility of organic materials is an outstanding feature for future flexible electronics.[4−7] Among the various types of organic electronic devices, organic resistive memory is being actively researched.[4−6,8−12] Organic resistive memory is similar to inorganic-based resistive random access memory (ReRAM), which typically uses oxide-based materials as an active layer in terms of the switching characteristics and device structure.[13−17] Organic resistive memory devices can be operated at a fast switching speed and a low voltage. Recently, 3-dimensional stacked organic memory devices have been demonstrated with the potential to open new possibilities for highly integrable organic devices.[10,11]

Graphene has been extensively investigated because of its excellent physical properties, such as its quantum transport effect,[18−21] high mobility,[19,22] electrochemical modulation,[23,24] and flexibility.[25,26] Graphene has been applied for various purposes: sensors,[22] biodevices,[27,28] channels for field-effect transistors,[29−33] the hole transport layer of organic solar cells,[34] active materials for memory devices,[35−40] or charge trapping layer[41] and electrodes for optoelectronic devices.[42−48] Because of the solution-processability of graphene, graphene is applied to an electrical device due to an easy fabrication process.[34,40,42,49] In particular, graphene has been widely adopted as a potential electrode for light-emitting diodes,[42,43,45] solar cells,[44,46−48] field-effect transistors,[50] touch pad displays,[25] and memory devices.[51]

Transparency and flexibility are essential requirements for the electrodes of electronic and photonic devices. Indium tin oxide (ITO) has been one of the most popular electrodes for a long time and, thus, has been used for a variety of device applications. However, the price of ITO is continually increasing due to the limited supply of indium,[52] and ITO is difficult to apply in flexible devices because of its brittle properties under bending.[2,48,53−55] On the other hand, graphene exhibits excellent durability under tension and compression,[56−58] and the reported transmittance of graphene is over 90%.[25,44,59] (Comparison results of optical image and sheet resistance of ITO and multilayer graphene (MLG) films on bending are provided in the Supporting Information.) Moreover, graphene maintains good interfacial contact with organic materials and shows a low contact resistance to organic materials.[60] We have previously reported that organic devices with graphene electrodes can have a low charge-injection barrier with enhanced mobility.[50] For this reason, graphene has been used as an electrode for various types of organic electronic devices,[50,60] including organic memory devices. Organic resistive memory devices with unpatterned graphene electrodes have

* Address correspondence to tlee@gist.ac.kr.

Received for review May 14, 2011 and accepted June 12, 2011.

Published online June 12, 2011
10.1021/nn201770s

shown write-once-read-many (WORM)-type memory characteristics with good performance parameters, although in previous studies, flexibility has not been demonstrated.[51]

Herein, we report the fabrication and testing of 8 × 8 array-type organic resistive memory devices with MLG top electrodes on a flexible substrate. The memory devices exhibited typical WORM switching characteristics, with a high ON/OFF ratio of over ~10^6, good cell-to-cell uniformity. The ON current of the WORM memory devices did not degrade substantially upon bending and bending cycling up to 10 000 times. A retention time over 10^4 s was sustained by the memory devices without substantial current fluctuation under bending.

RESULTS AND DISCUSSION

Figure 1 shows the fabrication process of the organic memory devices with transparent MLG top electrodes. Figure 1a shows the transferred MLG film on a 300-nm-thick SiO_2 wafer used to prepare the top electrodes of the memory devices. To form line patterns on the graphene electrodes, a 50-nm-thick Ni layer was deposited on the MLG film using a shadow mask. Subsequently, the unwanted graphene was removed by exposure to oxygen plasma, and the Ni mask patterns were then etched in aqueous iron chloride ($FeCl_3$) solution. The final patterned MLG electrodes are shown in Figure 1b. The patterned MLG electrodes were passivated with poly(methyl methacrylate) (PMMA) to minimize the film damage during the stripping of the MLG film from the substrate. The PMMA-coated graphene electrodes were stripped from the SiO_2 substrate by etching the SiO_2 layer with buffered oxide etchant (Figure 1c).

To form the organic active layer, a poly(ethylene terephthalate) (PET) substrate was cleaned by an ultrasonic cleaning process using acetone, methanol, and deionized water successively for 3 min each. To remove residual solvent from the PET substrate, the cleaned PET substrate was baked in a vacuum oven at 100 °C overnight. Al bottom electrodes were not formed well on the PET substrate without this prebaking process (see Figure S3 in the Supporting Information). After prebaking, 50-nm-thick Al bottom electrodes were deposited with a shadow mask (Figure 1d). As the active layer of the organic memory devices, biphenyltetracarboxylic acid dianhydride *p*-phenylene diamine (BPDA-PPD) as a polyimide (PI) precursor was dissolved in *N*-methyl-2-pyrrolidone (NMP) (BPDA-PPD:NMP solvent = 1:3 weight ratio), and 6-phenyl-C61 butyric acid methyl ester (PCBM) was dissolved in NMP at a concentration of 0.5 wt %. A PI:PCBM composite solution was prepared by blending the PI solution (2 mL) with the PCBM solution (0.5 mL). The Al surface on the PET substrate was exposed to UV−ozone treatment.[61] Then, the prepared PI:PCBM composite solution was spin-coated onto the prepared Al bottom electrodes on PET substrate at 500 rpm for 5 s and then at 2000 rpm

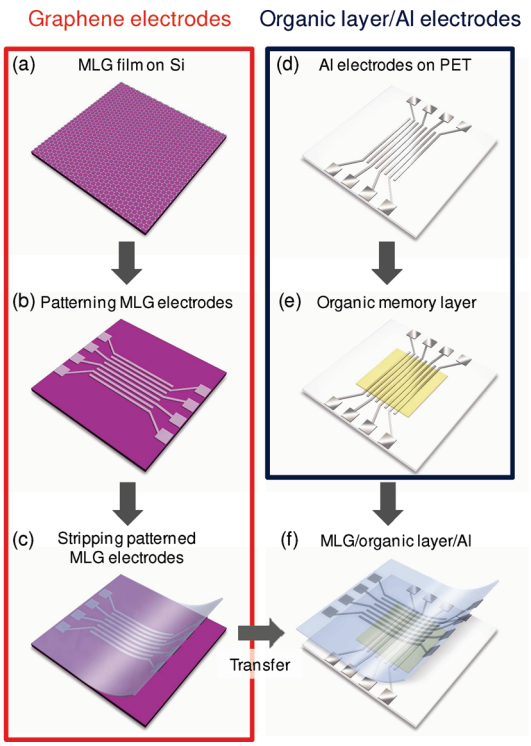

Figure 1. Fabrication process of flexible organic memory devices with transparent graphene top electrodes.

for 35 s (Figure 1e). The thickness of the PI:PCBM layer was measured to be ~30 nm based on cross-sectional transmission electron microscopy (TEM). To minimize parasitic leakage current during electrical characterization, the polymer layer on the Al pads was removed by methanol after soft baking at 60 °C. Then, the device was hard baked at 100 °C in a vacuum oven for 24 h to enhance the film uniformity and allow for the evaporation of residual solvent and thermal curing. Finally, the patterned MLG electrodes coated with PMMA (Figure 1c) were vertically aligned with bottom Al electrodes and transferred to the substrate (Figure 1f). PMMA was then removed using acetone from the MLG top electrodes. The optical images in Figure S1 of the Supporting Information show more details of the device fabrication process.

We synthesized graphene films by chemical vapor deposition on a Ni film-deposited SiO_2/Si substrate. Detailed information about the growth of the graphene films is provided in the Experimental Methods. Figure 2 panels a and b show an optical image and a Raman spectra of a MLG film from MLG/PI:PCBM/Al memory device structure on PET substrate, respectively. As shown in Figure 2b, the two intense peaks are attributed to the characteristic G band at ~1580 cm^{-1} and the 2D band at ~2700 cm^{-1}. The graphene film is multilayer graphene film because the G band is larger than the 2D band,[62] and the small D band intensity compared to the G band intensity indicates a low level of defects or local disorder in the MLG film.[44,45]

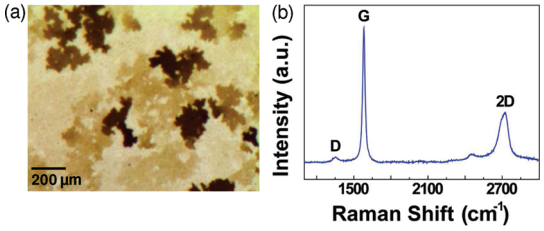

Figure 2. (a) Optical image of a MLG film and (b) Raman spectra of a MLG film from MLG/PI:PCBM/Al memory device structure on a PET substrate.

The sheet resistance of MLG film on a memory device was found to be ~270 Ω/□. From a separate measurement, the transmittance of MLG films was found to be ~92%. These characteristics of a MLG film will be appropriative for transparent electrodes.

Representative current−voltage (*I*−*V*) characteristics of an organic memory device are shown in Figure 3a. The current state of the memory device remained low (high-resistance state, HRS) at an initial low voltage but gradually increased as the applied voltage increased. At a voltage greater than ~4 V, the current state of the memory device increased abruptly and transformed into a high-current state (low-resistance state, LRS). During the sequential sweep, the device remained in an LRS, indicating a nonvolatile memory effect. Once the device achieved the LRS, we did not observe resistance recovery to the initial HRS, even above 15 V, which is known to be a characteristic of WORM-type memory.[63] In particular, the organic resistive memory showed a high ON/OFF ratio of over 10^6 at 0.3 V. Bias was applied to the MLG top electrodes in the electrical characterization of our devices. It is important to note that previous reports on memory devices using the same material (PI:PCBM) have shown rewritable switching characteristics.[5,9,10,64] However, the memory devices in our study showed WORM-type switching behavior. Although the switching mechanism is not understood clearly yet, but it seems that the resistive switching characteristics is associated with the charge-trapping mechanism.[5,9,10,64−68] Also, the memory switching behavior depends on the choice of electrodes and interface treatment between the active layer and electrodes.[13,14,17,61,64,69,70] WORM-type devices are good for saving important data without data loss. Note that a cross talk interference between memory cells can occur due to leakage current paths through neighboring cells with low resistances in array structures or an excess of current that may induce electrical damage. This phenomenon disturbs the reading process of the selected cells, which must be eliminated to enable practical memory application. To prevent this undesired cross talk problem, architectures involving switching control elements such as transistors[8] or diode[9] or blending active materials with ferroelectric materials[71] in organic memory array devices have been demonstrated. At the current stage, our

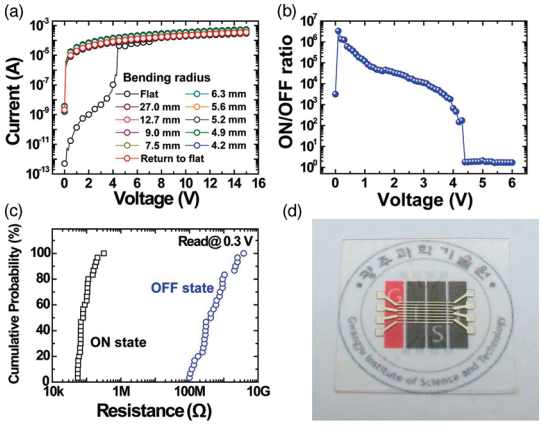

Figure 3. (a) *I*−*V* characteristics of an MLG/PI:PCBM/Al flexible organic memory device under different bending conditions; (b) ON/OFF ratio of a flat memory device; (c) cumulative probability data of flat memory devices; (d) optical image of flexible organic memory devices with transparent MLG top electrodes.

devices suffer from the cross talk phenomenon unless we can introduce switching control elements in the graphene−electrode flexible organic memory array devices.

We investigated the electrical characteristics of the memory devices under bending. Specifically, we bent our devices from a flat configuration (the substrate distance, the distance between two end points of the substrate, was 15.2 mm) to a radius of curvature of ~4.2 mm (the substrate distance was 11.0 mm). By decreasing the substrate distance, an arch shape was formed; that is, the devices became more bent. The maximum radius of curvature achieved in our study was ~4.2 mm (see Figure S4 of the Supporting Information). This high radius of curvature indicates greater flexibility than previously reported for flexible organic memory devices with an Al/PI:PCBM/Al structure, which results from the good flexibility of the MLG electrodes. As shown in Figure 3a, there were no significant current variations under bending. The maximum ON/OFF ratio of the memory devices under the flat condition was over 10^6 (Figure 3b).

The statistical cell-to-cell uniformity of memory devices is important for practical device application. The cumulative probability was analyzed using 30 randomly selected cells in the memory devices. Figure 3c shows the cumulative probability data of the MLG/PI:PCBM/Al

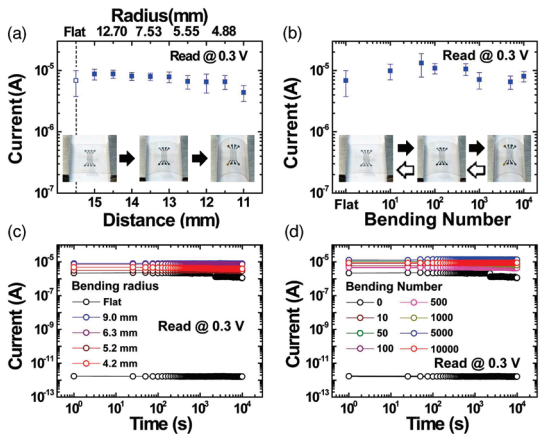

Figure 4. Statistical ON current distribution of flexible organic memory devices (a) under different bending conditions and (b) for different bending cycle numbers. Retention time of flexible memory devices under (c) different bending conditions and (d) bending cycles.

memory devices under the flat condition, which exhibited good cell-to-cell uniformity. The memory devices with MLG electrodes showed a narrow distribution in both the ON and OFF states. More importantly, the ON states were well separated from the OFF states, indicating that the memory margin was sufficient to distinguish each state.

Figure 3d shows an optical image of an organic memory device to demonstrate its transparency. The logo of our university placed behind the transparent organic memory device can be seen clearly. This transparency is due to the fact that the patterned MLG electrodes (the vertical electrodes shown in this image) exhibit excellent transmittance. Note that our device structure of MLG/PI:PCBM/Al on PET is not fully transparent because of Al bottom electrode. One would need both top and bottom graphene electrodes for fully transparent and flexible memory devices.

To evaluate the flexible organic memory devices in detail, their memory characteristics were analyzed under various bending conditions. Figure 4a shows the statistical ON current distribution from the flat to the maximum bending condition. The ON current remained stable without any substantial current fluctuation under the harsh bending conditions, as shown in Figure 4a. In addition to determining the bending tolerated, it is important to investigate how long the memory device can withstand bending cycling. Regardless of the bending condition, we found that the LRS current state was well maintained for up to 10 000 bending cycles (Figure 4b). In Figure 4b, one bending number (*x*-axis) denotes one cycle from the flat to the maximum bending condition (radius of curvature of ~4.2 mm) and back to the flat condition. For example, the data provided for a bending number of 10^4 indicates the LRS current state after the device had been bent to the maximum bending condition 10 000 times. The bending number was counted by an automated bending machine (see Figure S5 of the Supporting Information).

In memory devices, the data storage time is very important for useful device application. For this reason, the retention of performance was tested under each different bending condition, and we found that there was no significant variation in the LRS current state for over 10^4 s (Figure 4c). Figure 4d shows the retention time characteristics for the various bending cycle numbers. From cycles 0 to 10 000 times, the devices exhibited stable and reliable characteristics without any substantial current fluctuations for over 10^4 s.

CONCLUSION

In summary, we fabricated the 8 × 8 cross-bar array flexible organic memory devices using transparent multilayer graphene top electrodes on a PET substrate. The flexible memory devices exhibited typical write-once-read-many (WORM)-type memory characteristics with a high ON/OFF ratio of over ~10^6. The memory devices showed good cell-to-cell uniformity and reliable characteristics under various bending conditions and up to 10 000 bending cycles. The retention time of the memory devices was maintained over 10^4 s without any substantial fluctuation under bending and bending cycling. This demonstration of the performance of flexible organic memory devices using graphene electrodes provides an important step toward enabling future flexible and transparent device applications.

EXPERIMENTAL METHODS

Multilayer graphene (MLG) films were synthesized by chemical vapor deposition. First, a 300-nm-thick Ni film-deposited substrate (2 × 8 cm^2) was loaded into a quartz tube and preannealed at 300 °C under the flow of 200 sccm of Ar mixed with 4% H_2 for 30 min. Then, the temperature of the Ni substrate was raised, and the MLG film was grown at 900 °C by flowing 5 sccm of methane and 150 sccm of 4% H_2 in Ar at the same time for 5 min. To suppress thick film formation, Ni substrates with grown MLG films were rapidly cooled down after MLG film growth. The synthesized MLG films were transferred and applied as the top electrode of organic memory devices. All of the electrical properties of the fabricated memory devices were characterized using a Keithley 4200-SCS parameter analyzer in a N_2-filled glovebox.

Acknowledgment. This work was supported by the National Research Laboratory program, National Core Research Center grant, World Class University program of the Korean Ministry of Education, Science and Technology, the Program for Integrated Molecular Systems/GIST, and the IT R&D program of MKE/KEIT.

Supporting Information Available: Optical images of the organic memory devices during the device fabrication; comparison of ITO and MLG films under bending; the effect of preannealing of the PET substrate in a vacuum oven before Al

bottom electrode deposition; bending conditions and estimation of the radius of curvature; and photos of the bending machine. This material is available free of charge *via* the Internet at http://pubs.acs.org.

REFERENCES AND NOTES

1. Kim, J. Y.; Lee, K.; Coates, N. E.; Moses, D.; Nguyen, T.-Q.; Dante, M.; Heeger, A. J. Efficient Tandem Polymer Solar Cells Fabricated by All-Solution Processing. *Science* **2007**, *317*, 222–225.
2. Na, S.-I.; Kim, S.-S.; Jo, J.; Kim, D.-Y. Efficient and Flexible ITO-Free Organic Solar Cells Using Highly Conductive Polymer Anodes. *Adv. Mater.* **2008**, *20*, 4061–4067.
3. Singh, M.; Haverinen, H. M.; Dhagat, P.; Jabbour, G. E. Inkjet Printing-Process and Its Applications. *Adv. Mater.* **2010**, *22*, 673–685.
4. Ling, Q.-D.; Liaw, D.-J.; Zhu, C.; Chan, D. S.-H.; Kang, E.-T.; Neoh, K.-G. Polymer Electronic Memories: Materials, Devices and Mechanisms. *Prog. Polym. Sci.* **2008**, *33*, 917–978.
5. Ji, Y.; Cho, B.; Song, S.; Kim, T.-W.; Choe, M.; Kahng, Y. H.; Lee, T. Stable Switching Characteristics of Organic Nonvolatile Memory on a Bent Flexible Substrate. *Adv. Mater.* **2010**, *22*, 3071–3075.
6. Yang, Y.; Ouyang, J.; Ma, L.; Tseng, R. J.-H.; Chu, C.-W. Electrical Switching and Bistability in Organic/Polymeric Thin Films and Memory Devices. *Adv. Funct. Mater.* **2006**, *16*, 1001–1014.
7. Sekitani, T.; Yokota, T.; Zschieschang, U.; Klauk, H.; Bauer, S.; Takeuchi, K.; Takamiya, M.; Sakurai, T.; Someya, T. Organic Nonvolatile Memory Transistors for Flexible Sensor Arrays. *Science* **2009**, *326*, 1516–1519.
8. Kim, T.-W.; Choi, H.; Oh, S.-H.; Wang, G.; Kim, D.-Y.; Hwang, H.; Lee, T. One Transistor−One Resistor Devices for Polymer Nonvolatile Memory Applications. *Adv. Mater.* **2009**, *21*, 2497–2500.
9. Cho, B.; Kim, T.-W.; Song, S.; Ji, Y.; Jo, M.; Hwang, H.; Jung, G.-Y.; Lee, T. Rewritable Switching of One Diode−One Resistor Nonvolatile Organic Memory Devices. *Adv. Mater.* **2010**, *22*, 1228–1232.
10. Song, S.; Cho, B.; Kim, T.-W.; Ji, Y.; Jo, M.; Wang, G.; Choe, M.; Kahng, Y. H.; Hwang, H.; Lee, T. Three-Dimensional Integration of Organic Resistive Memory Devices. *Adv. Mater.* **2010**, *22*, 5048–5052.
11. Kwan, W. L.; Tseng, R. J.; Yang, Y. Multilayer Stackable Polymer Memory Devices. *Philos. Trans. R. Soc. A* **2009**, *367*, 4159–4167.
12. Scott, J. C.; Bozano, L. D. Nonvolatile Memory Elements Based on Organic Materials. *Adv. Mater.* **2007**, *19*, 1452–1463.
13. Sawa, A. Resistive Switching in Transition Metal Oxides. *Mater. Today* **2008**, *11*, 28–36.
14. Sawa, A.; Fujii, T.; Kawasaki, M.; Tokura, Y. Hysteretic Current−Voltage Characteristics and Resistance Switching at a Rectifying Ti/$Pr_{0.7}Ca_{0.3}MnO_3$ Interface. *Appl. Phys. Lett.* **2004**, *85*, 4073–4075.
15. Waser, R.; Aono, M. Nanoionics-Based Resistive Switching Memories. *Nat. Mater.* **2007**, *6*, 833–840.
16. Kwon, D.-H.; Kim, K. M.; Jang, J. H.; Jeon, J. M.; Lee, M. H.; Kim, G. H.; Li, X.-S.; Park, G.-S.; Lee, B.; Han, S.; Kim, M.; *et al.* Atomic Structure of Conducting Nanofilaments in TiO_2 Resistive Switching Memory. *Nat. Nanotechnol.* **2010**, *5*, 148–153.
17. Tsubouchi, K.; Ohkubo, I.; Kumigashira, H.; Oshima, M.; Matsumoto, Y.; Itaka, K.; Ohnishi, T.; Lippmaa, M.; Koinuma, H. High-Throughput Characterization of Metal Electrode Performance for Electric-Field-Induced Resistance Switching in Metal/$Pr_{0.7}Ca_{0.3}MnO_3$/Metal Structures. *Adv. Mater.* **2007**, *19*, 1711–1713.
18. Novoselov, K. S.; Geim, A. K.; Morozov, S. V.; Jiang, D.; Katsnelson, M. I.; Grigorieva, I. V.; Dubonos, S. V.; Firsov, A. A. Two-Dimensional Gas of Massless Dirac Fermions in Graphene. *Nature* **2005**, *438*, 197–200.
19. Bolotin, K. I.; Ghahari, F.; Shulman, M. D.; Stormer, H. L.; Kim, P. Observation of the Fractional Quantum Hall Effect in Graphene. *Nature* **2009**, *462*, 196–199.
20. Zhang, Y.; Tan, Y.-W.; Stormer, H. L.; Kim, P. Experimental Observation of the Quantum Hall Effect and Berry's Phase in Graphene. *Nature* **2005**, *438*, 201–204.
21. Novoselov, K. S.; Jiang, Z.; Zhang, Y.; Morozov, S. V.; Stormer, H. L.; Zeitler, U.; Maan, J. C.; Boebinger, G. S.; Kim, P.; Geim, A. K. Room-Temperature Quantum Hall Effect in Graphene. *Science* **2007**, *315*, 1379.
22. Fowler, J. D.; Allen, M. J.; Tung, V. C.; Yang, Y.; Kaner, R. B.; Weiller, B. H. Practical Chemical Sensors from Chemically Derived Graphene. *ACS Nano* **2009**, *3*, 301–306.
23. Geng, H.-Z.; Kim, K. K.; So, K. P.; Lee, Y. S.; Chang, Y.; Lee, Y. H. Effect of Acid Treatment on Carbon Nanotube-Based Flexible Transparent Conducting Films. *J. Am. Chem. Soc.* **2007**, *129*, 7758–7759.
24. Bunch, J. S.; van der Zande, A. M.; Verbridge, S. S.; Frank, I. W.; Tanenbaum, D. M.; Parpia, J. M.; Craighead, H. G.; McEuen, P. L. Electromechanical Resonators from Graphene Sheets. *Science* **2007**, *315*, 490–493.
25. Bae, S.; Kim, H.; Lee, Y.; Xu, X.; Park, J.-S.; Zheng, Y.; Balakrishnan, J.; Lei, T.; Kim, H. R.; Song, Y. I.; *et al.* Roll-to-roll Production of 30-inch. Graphene Films for Transparent Electrodes. *Nat. Nanotechnol.* **2010**, *5*, 574–578.
26. Kim, K. S.; Zhao, Y.; Jang, H.; Lee, S. Y.; Kim, J. M.; Kim, K. S.; Ahn, J.-H.; Kim, P.; Choi, J.-Y.; Hong, B. H. Large-Scale Pattern Growth of Graphene Films for Stretchable Transparent Electrodes. *Nature* **2009**, *457*, 706–710.
27. Qin, W.; Li, X.; Bian, W.-W.; Fan, X.-J.; Qi, J.-Y. Density Functional Theory Calculations and Molecular Dynamics Simulations of the Adsorption of Biomolecules on Graphene Surfaces. *Biomaterials* **2010**, *31*, 1007–1016.
28. Tang, Z.; Wu, H.; Cort, J. R.; Buchko, G. W.; Zhang, Y.; Shao, Y.; Aksay, I. A.; Liu, J.; Lin, Y. Constraint of DNA on Functionalized Graphene Improves its Biostability and Specificity. *Small* **2010**, *6*, 1205–1209.
29. Bai, J.; Zhong, X.; Jiang, S.; Huang, Y.; Duan, X. Graphene Nanomesh. *Nat. Nanotechnol.* **2010**, *5*, 190–194.
30. Yang, X.; Liu, G.; Balandin, A. A.; Mohanram, K. Triple-Mode Single-Transistor Graphene Amplifier and Its Applications. *ACS Nano* **2010**, *4*, 5532–5538.
31. Wang, H.; Wu, Y.; Cong, C.; Shang, J.; Yu, T. Hysteresis of Electronic Transport in Graphene Transistors. *ACS Nano* **2010**, *4*, 7221–7228.
32. Kim, B. J.; Jang, H.; Lee, S.-K.; Hong, B. H.; Ahn, J.-H.; Cho, J. H. High-Performance Flexible Graphene Field Effect Transistors with Ion Gel Gate Dielectrics. *Nano Lett.* **2010**, *10*, 3464–3466.
33. Jiao, L.; Zhang, L.; Wang, X.; Diankov, G.; Dai, H. Narrow Graphene Nanoribbons from Carbon Nanotubes. *Nature* **2009**, *458*, 877–880.
34. Li, S.-S.; Tu, K.-H.; Lin, C.-C.; Chen, C.-W.; Chhowalla, M. Solution-Processable Graphene Oxide as an Efficient Hole Transport Layer in Polymer Solar Cells. *ACS Nano* **2010**, *4*, 3169–3174.
35. Jeong, H. Y.; Kim, J. Y.; Kim, J. W.; Hwang, J. O.; Kim, J.-E.; Lee, J. Y.; Yoon, T. H.; Cho, B. J.; Kim, S. O.; Ruoff, R. S.; *et al.* Graphene Oxide Thin Films for Flexible Nonvolatile Memory Applications. *Nano Lett.* **2010**, *10*, 4381–4386.
36. Son, D. I.; Kim, T. W.; Shim, J. H.; Jung, J. H.; Lee, D. U.; Lee, J. M.; Park, W. I.; Choi, W. K. Flexible Organic Bistable Devices Based on Graphene Embedded in an Insulating Poly(methyl methacrylate) Polymer Layer. *Nano Lett.* **2010**, *10*, 2441–2447.
37. Sinitskii, A.; Dimiev, A.; Kosynkin, D. V.; Tour, J. M. Graphene Nanoribbon Devices Produced by Oxidative Unzipping of Carbon Nanotubes. *ACS Nano* **2010**, *4*, 5405–5413.
38. Sinitskii, A.; Tour, J. M. Lithographic Graphitic Memories. *ACS Nano* **2009**, *3*, 2760–2766.
39. Zhuang, X.-D.; Chen, Y.; Liu, G.; Li, P.-P.; Zhu, C.-X.; Kang, E.-T.; Noeh, K.-G.; Zhang, B.; Zhu, J.-H.; Li, Y.-X. Conjugated-Polymer-Functionalized Graphene Oxide: Synthesis and Nonvolatile Rewritable Memory Effect. *Adv. Mater.* **2010**, *22*, 1731–1735.
40. Liu, G.; Zhuang, X.; Chen, Y.; Zhang, B.; Zhu, J.; Zhu, C.-X.; Neoh, K.-G.; Kang, E.-T. Bistable Electrical Switching and Electronic Memory Effect in a Solution-Processable Graphene Oxide-Donor Polymer Complex. *Appl. Phys. Lett.* **2009**, *95*, 253301.
41. Kim, T.-W.; Gao, Y.; Acton, O.; Yip, H.-L.; Ma, H.; Chen, H.; Jen, A. K.-Y. Graphene Oxide Nanosheets Based Organic Field

Effect Transistor for Nonvolatile Memory Applications. *Appl. Phys. Lett.* **2010**, *97*, 023310.
42. Wu, J.; Agrawal, M.; Becerril, H. A.; Bao, Z.; Liu, Z.; Chen, Y.; Peumans, P. Organic Light-Emitting Diodes on Solution-Processed Graphene Transparent Electrodes. *ACS Nano* **2010**, *4*, 43–48.
43. Matyba, P.; Yamaguchi, H.; Eda, G.; Chhowalla, M.; Edman, L.; Robinson, N. D. Graphene and Mobile Ions: The Key to All-Plastic, Solution-Processed Light-Emitting Devices. *ACS Nano* **2010**, *4*, 637–642.
44. Choe, M.; Lee, B. H.; Jo, G.; Park, J.; Park, W.; Lee, S.; Hong, W.-K.; Seong, M.-J.; Kahng, Y. H.; Lee, K.; *et al*. Efficient Bulk-Heterojunction Photovoltaic Cells with Transparent Multi-Layer Graphene Electrodes. *Org. Electron* **2010**, *11*, 1864–1869.
45. Jo, G.; Choe, M.; Cho, C.-Y.; Kim, J. H.; Park, W.; Lee, S.; Hong, W.-K.; Kim, T.-W.; Park, S.-J.; Hong, B. H.; *et al*. Large-Scale Patterned Multilayer Graphene Films as Transparent Conducting Electrodes for GaN Light-Emitting Diodes. *Nanotechnology* **2010**, *21*, 175201.
46. Tung, V. C.; Chen, L.-M.; Allen, M. J.; Wassei, J. K.; Nelson, K.; Kaner, R. B.; Yang, Y. Low-Temperature Solution Processing of Graphene-Carbon Nanotube Hybrid Materials for High-Performance Transparent Conductors. *Nano Lett.* **2009**, *9*, 1949–1955.
47. Yin, Z.; Sun, S.; Salim, T.; Wu, S.; Huang, X.; He, Q.; Lam, Y. M.; Zhang, H. Organic Photovoltaic Devices Using Highly Flexible Reduced Graphene Oxide Films as Transparent Electrodes. *ACS Nano* **2010**, *4*, 5263–5268.
48. Gomez De Arco, L.; Zhang, Y.; Schlenker, C. W.; Ryu, K.; Thompson, M. E.; Zhou, C. Continuous, Highly Flexible, and Transparent Graphene Films by Chemical Vapor Deposition for Organic Photovoltaics. *ACS Nano* **2010**, *4*, 2865–2873.
49. Green, A. A.; Hersam, M. C. Solution Phase Production of Graphene with Controlled Thickness *via* Density Differentiation. *Nano Lett.* **2009**, *9*, 4031–4036.
50. Lee, S.; Jo, G.; Kang, S.-J.; Wang, G.; Choe, M.; Park, W.; Kim, D.-Y.; Kahng, Y. H.; Lee, T. Enhanced Charge Injection in Pentacene Field-Effect Transistors with Graphene Electrodes. *Adv. Mater.* **2011**, *23*, 100–105.
51. Liu, J.; Yin, Z.; Cao, X.; Zhao, F.; Lin, A.; Xie, L.; Fan, Q.; Boey, F.; Zhang, H.; Huang, W. Bulk Heterojunction Polymer Memory Devices with Reduced Graphene Oxide as Electrodes. *ACS Nano* **2010**, *4*, 3987–3992.
52. Forrest, S. R. The Path to Ubiquitous and Low-Cost Organic Electronic Appliances on Plastic. *Nature* **2004**, *428*, 911–918.
53. Lee, B. H.; Park, S. H; Back, H.; Lee, K. Novel Film-Casting Method for High-Performance Flexible Polymer Electrodes. *Adv. Funct. Mater.* **2011**, *21*, 487–493.
54. Boehme, M.; Charton, C. Properties of ITO on PET Film in Dependence on the Coating Conditions and Thermal Processing. *Surf. Coat. Technol.* **2005**, *200*, 932–935.
55. Chen, Z.; Cotterell, B.; Wang, W.; Guenther, E.; Chua, S.-J. A Mechanical Assessment of Flexible Optoelectronic Devices. *Thin Solid Films* **2001**, *394*, 202–206.
56. Frank, O.; Tsoukleri, G.; Parthenios, J.; Papagelis, K.; Riaz, I.; Jalil, R.; Novoselov, K. S.; Galiotis, C. Compression Behavior of Single-Layer Graphenes. *ACS Nano* **2010**, *4*, 3131–3138.
57. Tsoukleri, G.; Parthenios, J.; Papagelis, K.; Jalil, R.; Ferrari, A. C.; Geim, A. K.; Novoselov, K. S.; Galiotis, C. Subjecting a Graphene Monolayer to Tension and Compression. *Small* **2009**, *5*, 2397–2402.
58. Yu, T.; Ni, Z.; Du, C.; You, Y.; Wang, Y.; Shen, Z. Raman Mapping Investigation of Graphene on Transparent Flexible Substrate: The Strain Effect. *J. Phys. Chem. C* **2008**, *112*, 12602–12605.
59. Li, X.; Zhu, Y.; Cai, W.; Borysiak, M.; Han, B.; Chen, D.; Piner, R. D.; Colombo, L.; Ruoff, R. S. Transfer of Large-Area Graphene Films for High-Performance Transparent Conductive Electrodes. *Nano Lett.* **2009**, *9*, 4359–4363.
60. Lee, C.-G.; Park, S.; Ruoff, R. S.; Dodabalapur, A. Integration of Reduced Graphene Oxide into Organic Field-Effect Transistors as Conducting Electrodes and as a Metal Modification Layer. *Appl. Phys. Lett.* **2009**, *95*, 023304.
61. Verbakel, F.; Meskers, S. C. J.; Janssen, R. A. J.; Gomes, H. L.; Cölle, M.; Büchel, M.; de Leeuw, D. M. Reproducible Resistive Switching in Nonvolatile Organic Memories. *Appl. Phys. Lett.* **2007**, *91*, 192103.
62. Li, X.; Cai, W.; An, J.; Kim, S.; Nah, J.; Yang, D.; Piner, R.; Velamakanni, A.; Jung, I.; Tutuc, E.; *et al*. Large-Area Synthesis of High-Quality and Uniform Graphene Films on Copper Foils. *Science* **2009**, *324*, 1312–1314.
63. Möller, S.; Perlov, C.; Jackson, W.; Taussig, C.; Forrest, S. R. A Polymer/Semiconductor Write-Once Read-Many-Times Memory. *Nature* **2003**, *426*, 166–169.
64. Cho, B.; Song, S.; Ji, Y.; Lee, T. Electrical Characterization of Organic Resistive Memory with Interfacial Oxide Layers Formed by O_2 Plasma Treatment. *Appl. Phys. Lett.* **2010**, *97*, 063305.
65. Cho, B.-O.; Yasue, T.; Yoon, H.; Lee, M.-S.; Yeo, I.-S.; Chung, U.-I.; Moon, J.-T.; Ryu, B.-I. Thermally Robust Multilayer Nonvolatile Polymer Resistive Memory. *IEEE Int. Electron. Devices Meet. Technol. Dig.* 2006, DOI: 10.1109/IEDM.2006.346729, pp 1-4.
66. Simmons, J. G.; Verderber, R. R. New Conduction and Reversible Memory Phenomena in Thin Insulating Films. *Proc. R. Soc. London. , Ser. A* **1967**, *301*, 77–102.
67. Bozano, L. D.; Kean, B. W.; Deline, V. R.; Salem, J. R.; Scott, J. C. Mechanism for Bistability in Organic Memory Elements. *Appl. Phys. Lett.* **2004**, *84*, 607–609.
68. Bozano, L. D.; Kean, B. W.; Beinhoff, M.; Carter, K. R.; Rice, P. M.; Scott, J. C. Organic Materials and Thin-Film Structures for Cross-Point Memory Cells Based on Trapping in Metallic Nanoparticles. *Adv. Funct. Mater.* **2005**, *15*, 1933–1939.
69. Mukherjee, B.; Pal, A. J. Tuning of Electrical Bistability in Organic Devices Through Electrochemical Potential of Metal Contacts. *Org. Electron* **2006**, *7*, 249–255.
70. Linn, E.; Rosezin, R.; Kügeler, C.; Waser, R. Complementary Resistive Switches for Passive Nanocrossbar Memories. *Nat. Mater.* **2010**, *9*, 403–406.
71. Asadi, K.; de Leeuw, D. M.; de Boer, B.; Blom, P. W. M. Organic Nonvolatile Memories from Ferroelectric Phase-Separated Blends. *Nat. Mater.* **2008**, *7*, 547–550.